

## Supporting Information

### Asymmetric D-A-D' Scaffold Inducing Distinct Mechanochromic Luminescence

Huifang Yang<sup>a</sup>, Zhiyuan Fu<sup>b</sup>, Sai Wang<sup>a</sup>, Haichao Liu<sup>c</sup>, Jianwei Zhou<sup>a</sup>, Kai Wang <sup>\*b</sup>,  
Xiugang Wu<sup>\*a</sup>, Bing Yang<sup>c</sup>, Bo Zou<sup>b</sup>, Weiguo Zhu<sup>\*a</sup>

*<sup>a</sup>School of Materials Science and Engineering, Jiangsu Collaboration Innovation Center of Photovoltaic Science and Engineering, Jiangsu Engineering Laboratory of Light-Electricity-Heat Energy-Converting Materials and Applications, National Experimental Demonstration Center for Materials Science and Engineering, Changzhou University, Changzhou 213164, P. R. China*

*<sup>b</sup>State Key Laboratory of Superhard Materials, College of Physics, Jilin University, Changchun 130012, P. R. China*

*<sup>c</sup>State Key Laboratory of Supramolecular Structure and Materials, College of Chemistry, Jilin University, Changchun 130012, P. R. China*

*\*To whom correspondence should be addressed. Email:*

*(W. Z.) [zhuwg18@126.com](mailto:zhuwg18@126.com)*

# Table of Contents

## 1. Experimental Procedures

Structural characterization

General Measurements

Photophysical measurements

Single crystal X-ray diffraction (XRD) data

Pressure-dependent experiment of crystal

## 2. Synthetic Details

Synthesis of CzPL-PTZ

Synthesis of CzPL-tDPA

## 3. Supplementary Figures S1-S26 and Tables S1-S7

## 4. References

## 1. Experimental Procedures

**Structural characterization:** All the reagents and solvents used for the synthesis were purchased from Aladdin and Energy companies without further purification. NMR spectra were recorded on a Bruker AVANCE spectrometer with tetramethyl silane as the internal standard. The Mass spectra were recorded on the Bruker Biflex III MALDI-TOF.

**General Measurements:** Thermogravimetric analysis (TGA) was conducted under nitrogen atmosphere at a heating of rate 10 °C/min performed using a NETZSCH STA449F5 Jupiter Synchronous thermal analyzer. Cyclic voltammetry (CV) was measured on a CHI660D electro-chemical workstation with three-electrode system, in which glassy carbon electrode, Pt wire electrode and Ag/AgCl electrode as working electrode, counter electrode and reference electrode, respectively. The supporting electrolyte used was 0.1 M tetrabutylammonium hexafluorophosphate (Bu<sub>4</sub>NPF<sub>6</sub>) solution in dry acetonitrile under a nitrogen atmosphere using ferrocene (Fc) as the calibrant. The potential of Fc/Fc<sup>+</sup> vs Ag/AgCl electrode was measured to be 0.42 V. Highest occupied molecular orbital (HOMO) energy level was determined from the onset potential of oxidation by cyclic voltammetry,  $E_{\text{HOMO}} = -(E_{\text{OX}} + 4.38)$ ; while lowest unoccupied molecular orbital (LUMO) energy level can be calculated using  $E_{\text{HOMO}}$  and optical band gap ( $E_g$ ),  $E_{\text{LUMO}} = E_{\text{HOMO}} + E_g$ .<sup>1-2</sup>

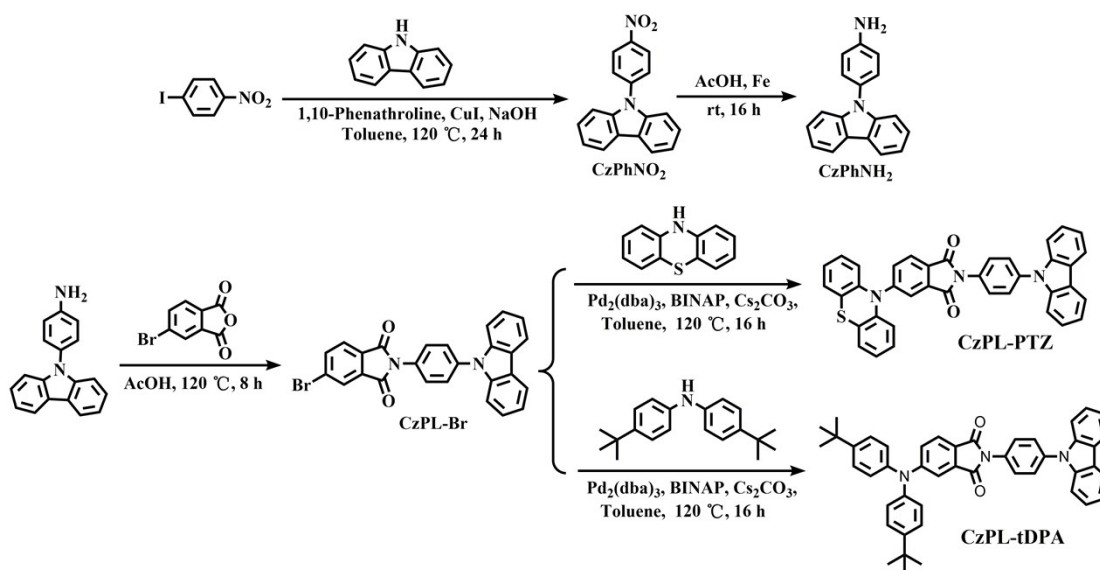
**Photophysical measurements:** Ultraviolet-visible (UV-Vis) spectra were recorded by a Shimadzu UV-2600 spectrophotometer. Photoluminescence (PL) spectra were carried out with FLS980 spectrometer. Photoluminescence quantum yield ( $\Phi_f$ ) were measured using an integrating sphere apparatus. The preparation of solid film is to dissolve the solid sample in chloroform (3 mg/mL) and spin coating on the quartz slice for 30 s at the speed of 3000 r/min on the spin coater.

**Single crystal X-ray diffraction (XRD) data:** The crystals were prepared by vacuum sublimation in nitrogen atmosphere. The diffraction experiments were carried out on a Rigaku R-AXIS RAPID diffractometer equipped with a Mo-K $\alpha$  and control Software using the RAPID AUTO. The crystal structures were solved with direct methods and

refined with a full-matrix least-squares technique using the SHELXS programs.

**Pressure-dependent experiment of crystal:** A symmetric diamond anvil cell (DAC) with 400  $\mu\text{m}$  diameter culet diamonds was used in high-pressure fluorescence and absorption experiments. The tiny crystal was placed in the hole (diameter: 130  $\mu\text{m}$ ) of a T301 steel gasket, and silicone oil was used as a pressure transmitting medium (PTM). The *in situ* steady-state PL measurement under high pressure was performed on an Ocean Optics QE65000 spectrometer in the reflection mode. The 355 nm line of violet diode laser with a spot size of 20 mm and a power of 10 mW was used as the excitation source. The *in situ* high-pressure absorption spectra were recorded by an optical fiber spectrometer (Ocean Optics, QE65000). The real optical photographs were obtained by using a Nikon Ti-U microscope equipped with a digital color camera.

## 2. Synthetic Details



**Scheme S1.** Synthesis route of CzPL-PTZ and CzPL-tDPA.

### Synthesis of CzPhNO<sub>2</sub>

A flask was charged with 1-iodo-4-nitrobenzene (5.00 g, 20.08 mmol), carbazole (3.36 g, 20.08 mmol), CuI (0.76 g, 4.02 mmol), NaOH (4.02 g, 100.40 mmol), 1,10-phenanthroline (0.72 g, 4.02 mmol) and toluene (50 mL). The mixture was degassed and stirred at 120 °C under nitrogen for 24 h. After cooling to room temperature, the mixture was washed with distilled water and then extracted with dichloromethane. The

organic phase was dried with anhydrous sodium sulfate and filtered. The resulting crude was purified by silica gel column chromatography with dichloromethane/petroleum ( $v/v = 1:3$ ) as eluent to obtain the yellow solid powder CzPhNO<sub>2</sub> in a yield of 82.05% (4.75 g). <sup>1</sup>H NMR (400 MHz, CDCl<sub>3</sub>)  $\delta$  8.49 (d,  $J = 9.0$  Hz, 2H), 8.15 (d,  $J = 7.7$  Hz, 2H), 7.81 (d,  $J = 8.9$  Hz, 2H), 7.54 – 7.42 (m, 4H), 7.35 (t,  $J = 6.9$  Hz, 2H).

### Synthesis of CzPhNH<sub>2</sub>

The mixture of CzPhNO<sub>2</sub> (4.00 g, 13.87 mmol), Fe (3.85 g, 69.35 mmol) and 60 mL acetic acid was placed in a flask at 0 °C. After 30 minutes, the mixture was transferred to room temperature for 16 h. Pouring the mixture into 150 mL ice water, the gray-white precipitation was filtered. Then the solid was dissolved in DCM, and the mixture was filtered. The solvent was removed by rotary evaporation, a brown viscous liquid CzPhNH<sub>2</sub> was obtained in a yield of 98% (3.5 g).

### Synthesis of CzPL-Br

A flask was charged with CzPhNH<sub>2</sub> (2.00 g, 7.74 mmol), 5-bromoisobenzofuran-1,3-dione (1.76 g, 7.74 mmol) and acetic acid (30 mL). The mixture was degassed and stirred at 120 °C under nitrogen for 8 h. After cooling to room temperature, the mixture was poured into 150 mL ice water and solid precipitation was formed. The precipitation was filtered and dried to obtain a yellow solid CzPL-Br in a yield of 96.3% (3.47 g). <sup>1</sup>H NMR (400 MHz, CDCl<sub>3</sub>)  $\delta$  8.15 (d,  $J = 7.2$  Hz, 3H), 7.97 (d,  $J = 7.9$  Hz, 1H), 7.87 (d,  $J = 7.9$  Hz, 1H), 7.72 (q,  $J = 8.7$  Hz, 4H), 7.50 (d,  $J = 8.2$  Hz, 2H), 7.44 (t,  $J = 7.6$  Hz, 2H), 7.31 (t,  $J = 7.4$  Hz, 2H).

### Synthesis of CzPL-PTZ

A flask was charged with CzPL-Br (1.00 g, 2.14 mmol), phenothiazine (0.51 g, 2.57 mmol), Pd<sub>2</sub>(dba)<sub>3</sub> (0.078 g, 0.086 mmol), 2,2'-bis(diphenylphosphino)-1,1'-binaphthalene (BINAP) (0.16 g, 0.26 mmol), Cs<sub>2</sub>CO<sub>3</sub> (2.79 g, 8.56 mmol) and toluene (30 mL). The mixture was degassed and stirred at 120 °C under nitrogen for 16 h. After cooling to room temperature, the mixture was concentrated. The resulting crude was purified by silica gel column chromatography with dichloromethane/ petroleum ( $v/v = 2:3$ ) as eluent to obtain the yellow solid powder in a yield of 56.80% (0.71 g). The product was purified by vacuum sublimation to give pale yellow-green crystal. <sup>1</sup>H NMR (500 MHz,

CDCl<sub>3</sub>)  $\delta$  8.15 (d,  $J$  = 7.7 Hz, 2H), 7.76 (d,  $J$  = 8.5 Hz, 1H), 7.68 (q,  $J$  = 8.8 Hz, 4H), 7.55 – 7.48 (m, 7H), 7.43 (t,  $J$  = 7.1 Hz, 4H), 7.34 – 7.28 (m, 5H). <sup>13</sup>C NMR (126 MHz, CDCl<sub>3</sub>)  $\delta$  167.10, 151.93, 140.72, 136.97, 134.57, 130.86, 129.29, 127.79, 127.47, 126.95, 126.07, 125.38, 123.49, 120.32, 120.16, 119.52, 109.88. TOF-MS (C<sub>38</sub>H<sub>23</sub>N<sub>3</sub>O<sub>2</sub>S): m/z 585.266.

### Synthesis of CzPL-tDPA

Following the same synthetic approach for **CzPL-PTZ**, the reaction of CzPL-Br (1.00 g, 2.14 mmol), bis(4-(*tert*-butyl)phenyl)amine (0.72 g, 2.56 mmol), Pd<sub>2</sub>(dba)<sub>3</sub> (0.078 g, 0.086 mmol), BINAP (0.16 g, 0.26 mmol), Cs<sub>2</sub>CO<sub>3</sub> (2.79 g, 8.56 mmol) and toluene (30 mL) was conducted to prepare **CzPL-tDPA** as yellow powder in a yield of 76.90% (1.10 g). Then the product was purified by vacuum sublimation to give blue-green crystal. <sup>1</sup>H NMR (500 MHz, CDCl<sub>3</sub>)  $\delta$  8.15 (d,  $J$  = 7.7 Hz, 2H), 7.73 – 7.66 (m, 5H), 7.51 (d,  $J$  = 8.2 Hz, 2H), 7.47 – 7.37 (m, 7H), 7.30 (t,  $J$  = 7.4 Hz, 2H), 7.20 (dd,  $J$  = 8.4, 2.2 Hz, 1H), 7.15 – 7.11 (m, 4H), 1.35 (s, 19H). <sup>13</sup>C NMR (126 MHz, CDCl<sub>3</sub>)  $\delta$  167.56, 167.08, 154.50, 148.82, 142.94, 140.72, 136.86, 133.81, 131.04, 127.78, 127.45, 126.95, 126.02, 125.12, 123.48, 122.81, 120.70, 120.32, 120.15, 113.25, 109.91, 34.59, 31.40. TOF-MS (C<sub>46</sub>H<sub>41</sub>N<sub>3</sub>O<sub>2</sub>): m/z 667.383.

### 3. Supplementary Figures and Tables

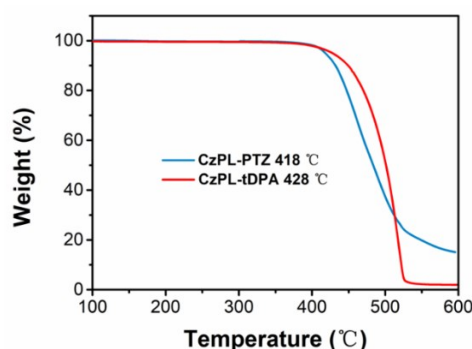


**Figure S1** TGA curves of **CzPL-PTZ** and **CzPL-tDPA** under N<sub>2</sub> atmosphere.

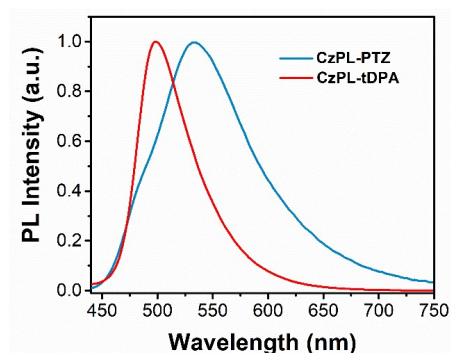


**Figure S2** PL spectra of CzPL-PTZ and CzPL-tDPA in crystal.

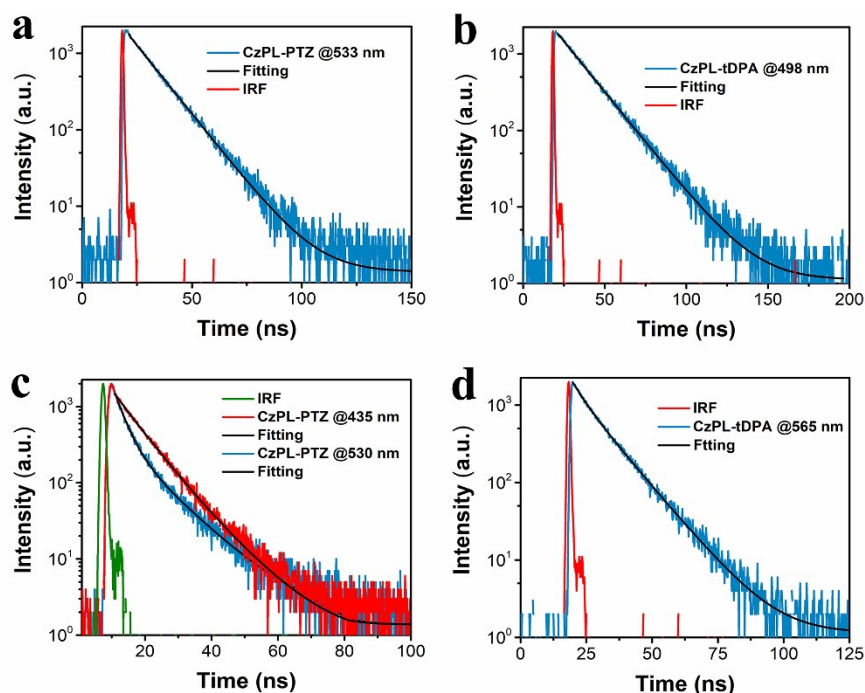


**Figure S3** PL decay curves of CzPL-PTZ and CzPL-tDPA in crystals and toluene solution ( $10^{-5}$  M), respectively (The excitation wavelength is 365 nm and the pulse width is 500 ns).

**Table S1** Transient PL decay data of CzPL-PTZ and CzPL-tDPA in crystals and toluene solution ( $10^{-5}$  M).

Compound	State	$\lambda_{em}$ (nm)	$\tau_1$ (ns)	$\tau_2$ (ns)	$A_1$ (%)	$A_2$ (%)	$\langle\tau\rangle$ (ns)	$\chi^2$
CzPL-PTZ	Crystal	533	0.20	12.09	0.16	99.84	12.07	0.9976
	Tol ( $10^{-5}$ M)	435	3.01	10.59	53.78	46.22	6.51	1.2022
		530	6.84	11.16	68.81	31.19	8.19	1.0612

<b>CzPL-tDPA</b>	Crystal	498	10.00	16.56	2.02	97.98	16.56	0.9233
	Tol (10 <sup>-5</sup> M)	565	4.51	10.92	14.43	85.57	10.00	0.9537

The transient PL decay data were fitted by multiple-exponential function and the mean fluorescence lifetimes ( $\langle\tau\rangle$ ) were calculated by  $\langle\tau\rangle = \Sigma A_i \tau_i^2 / \Sigma A_i \tau_i$ , where  $A_i$  is the pre-exponential for lifetime  $\tau_i$ . In addition,  $\chi^2$  is the residual.

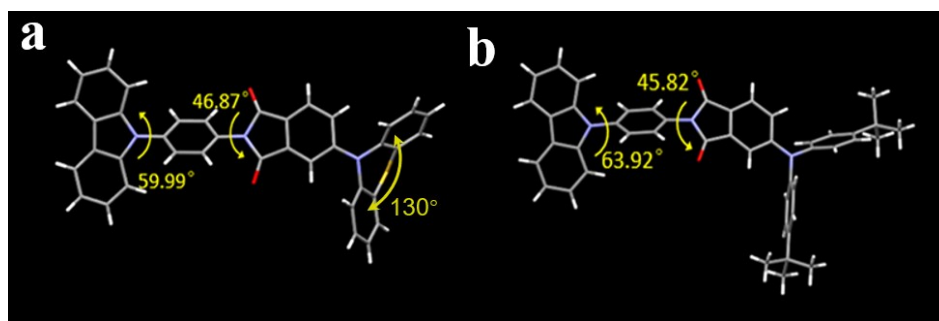


**Figure S4** Single crystal structures of (a) CzPL-PTZ and (b) CzPL-tDPA.

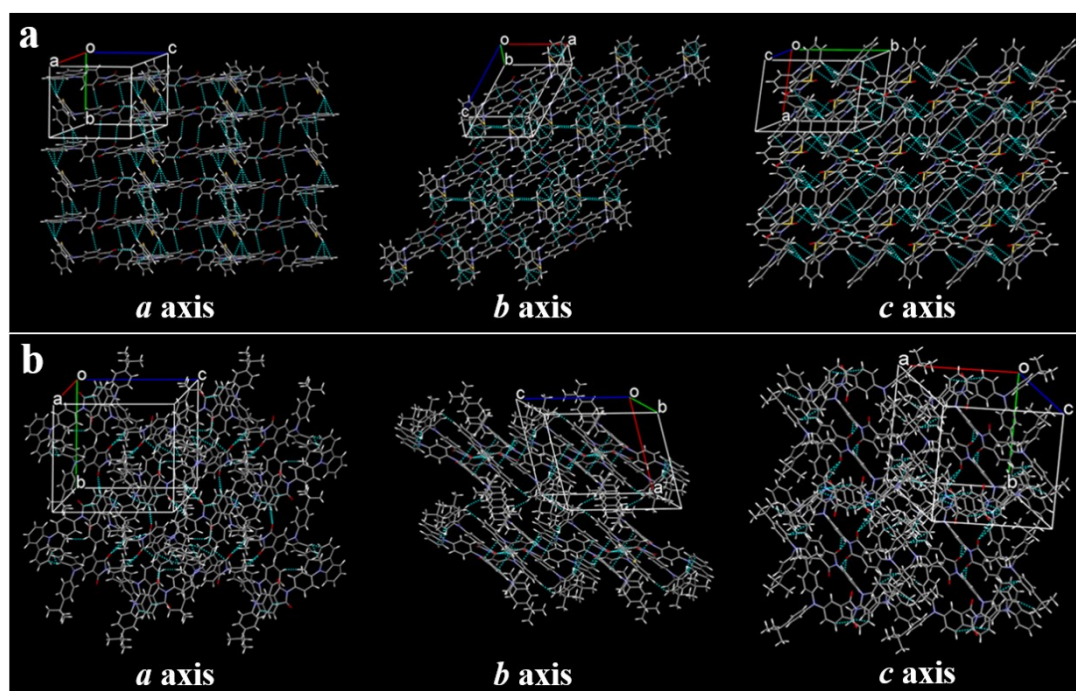


**Figure S5** Views of molecular packing of crystals CzPL-PTZ (a) and crystal CzPL-tDPA (b) from *a* axis, *b* axis and *c* axis. Green lines represent the intermolecular interactions.

**Table S2** Summary of the crystal data for **CzPL-PTZ** and **CzPL-tDPA**.

Identification code	<b>CzPL-PTZ</b>	<b>CzPL-tDPA</b>
Empirical formula	C <sub>38</sub> H <sub>23</sub> N <sub>3</sub> O <sub>2</sub> S	C <sub>46</sub> H <sub>41</sub> N <sub>3</sub> O <sub>2</sub>
CCDC	2071819	2071820
Formula weight	585.65	667.82
Temperature / K	160.0	170.0
Crystal system	triclinic	monoclinic
Space group	P -1	P2 <sub>1</sub> / c
a/Å	10.2420 (3)	14.4680(7)
b/Å	12.2042 (4)	15.4885(7)
c/Å	12.5581 (4)	16.8014(7)
$\alpha$ /°	94.766 (1)	90
$\beta$ /°	112.178 (1)	105.651(2)
$\gamma$ /°	101.356(1)	90
Volume/Å <sup>3</sup>	1403.34(6)	3625.4(3)
Z	2	4
$\rho$ calc g/cm <sup>3</sup>	1.386	1.224
$\mu$ /mm <sup>-1</sup>	0.158	0.075
F (000)	608.0	1416.0
Crystal size/mm <sup>3</sup>	0.15 × 0.08 × 0.05	0.15 × 0.08 × 0.05
Radiation	MoK $\alpha$ ( $\lambda$ = 0.71073)	MoK $\alpha$ ( $\lambda$ = 0.71073)
2 $\Theta$ range for data collection/°	4.426 to 55.046	3.932 to 50.698

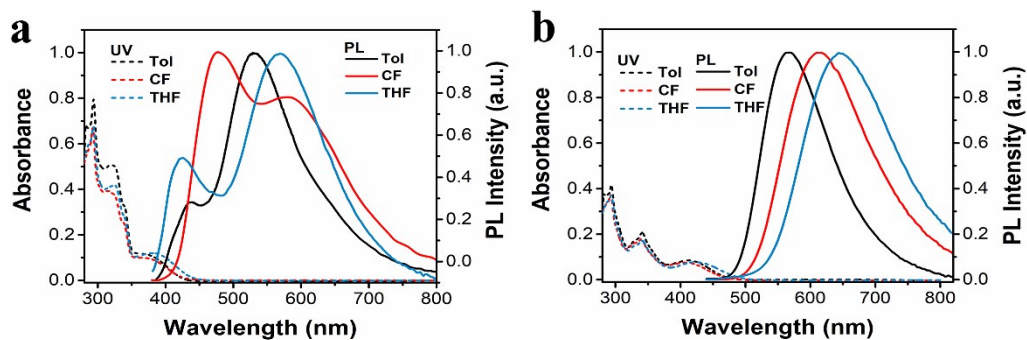


**Figure S6** UV-vis and PL spectra of (a) CzPL-PTZ and (b) CzPL-tDPA in different solvents ( $1.0 \times 10^{-5}$  M) (toluene (Tol), chloroform (CF) and tetrahydrofuran (THF)).

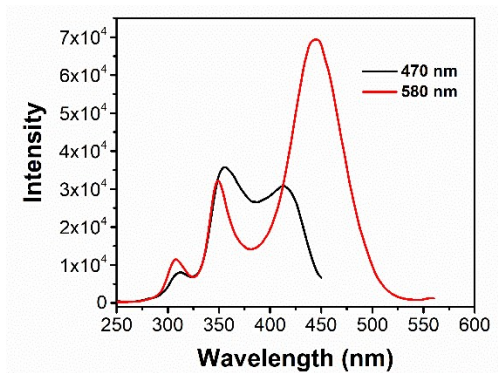


**Figure S7** Excitation spectra of CzPL-PTZ at 480 nm and 560 nm in CF solvent ( $1.0 \times 10^{-5}$  M).

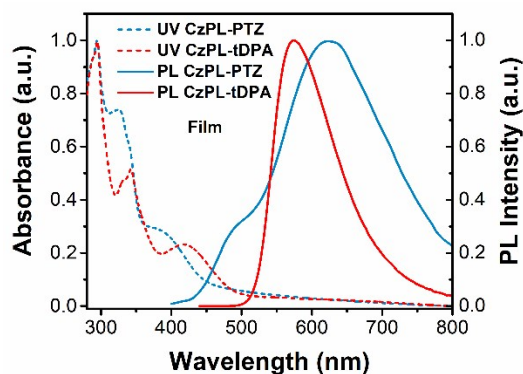


**Figure S8** UV-vis and PL spectra of **CzPL-PTZ** and **CzPL-tDPA** in films.

**Table S3** Summary photophysical data of **CzPL-PTZ** and **CzPL-tDPA** in different solvents and films.

	$\lambda_{\text{abs}}$ (nm)				$\lambda_{\text{em}}$ (nm)			
	Tol	CF	THF	Film	Tol	CF	THF	Film
<b>CzPL-PTZ</b>	294/323/ 375	293/326/ 385	290/320/ 374	295/328/ 390	435/ 530	476/ 583	424/ 570	489/ 626
<b>CzPL-tDPA</b>	293/341/ 434	293/341/ 427	292/339/ 410	294/332/ 420	565	612	645	575

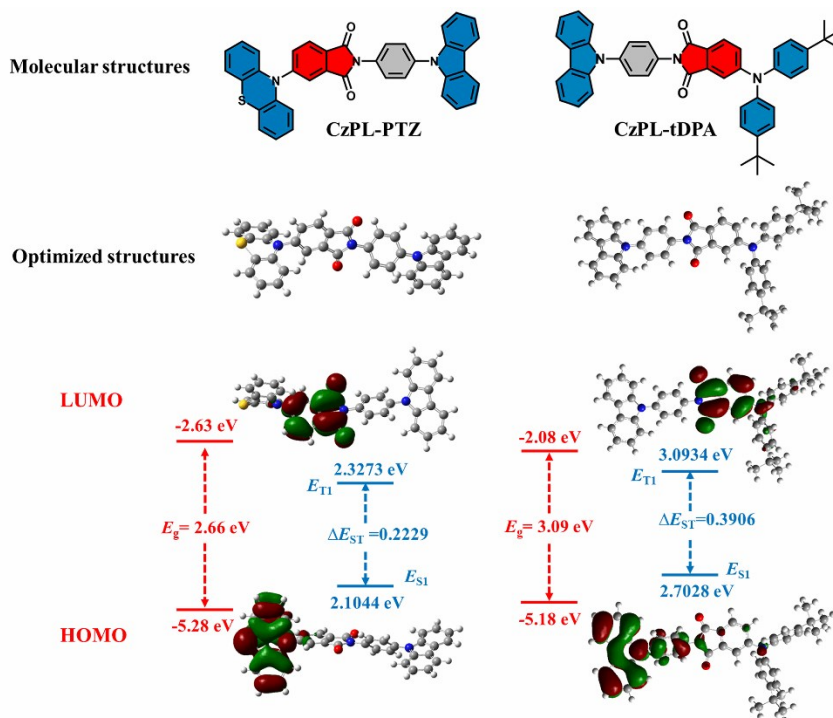


**Figure S9** Molecular structures, optimized ground-state ( $S_0$ ) structures, HOMO and LUMO distributions, and energy levels of HOMOs/LUMOs, energy gap ( $E_g$ ) of **CzPL-**

**PTZ** and **CzPL-tDPA** based on DFT at the B3LYP/6-31G(d)/LanL2DZ level. Calculated energy levels of first singlet ( $S_1$ ) state ( $E_{S1}$ ) and first triplet ( $T_1$ ) state ( $E_{T1}$ ), and splitting energies of  $S_1$  and  $T_1$  ( $\Delta E_{ST}$ ) of **CzPL-PTZ** and **CzPL-tDPA** based on TD-DFT at the same level are listed.

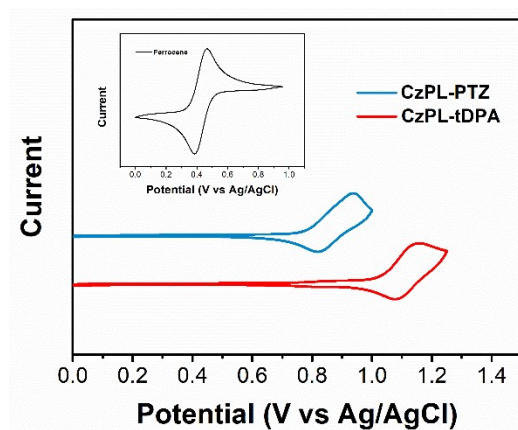


**Figure S10** Cyclic voltammetry curves of **CzPL-PTZ** and **CzPL-tDPA** in  $\text{CH}_3\text{CN}$ .

**Table S4** Summary data of **CzPL-PTZ** and **CzPL-tDPA** HOMO and LUMO energy level.

Compound	$E_{\text{HOMO}}^{\text{[a]}}$ (eV)	$E_{\text{LUMO}}^{\text{[a]}}$ (eV)	$E_{\text{g}}^{\text{[b]}}$ (eV)
<b>CzPL-PTZ</b>	-5.16	-2.04	3.12
<b>CzPL-tDPA</b>	-5.41	-2.48	2.93

[a]  $E_{\text{HOMO}}$  was determined from the half-wave potentials of the oxidation reduction curves.  $E_{\text{LUMO}} = E_{\text{HOMO}} + E_{\text{g}}$ .

[b] Energy gap ( $E_{\text{g}}$ ) was obtained from the onsets of UV-Vis absorption spectra.

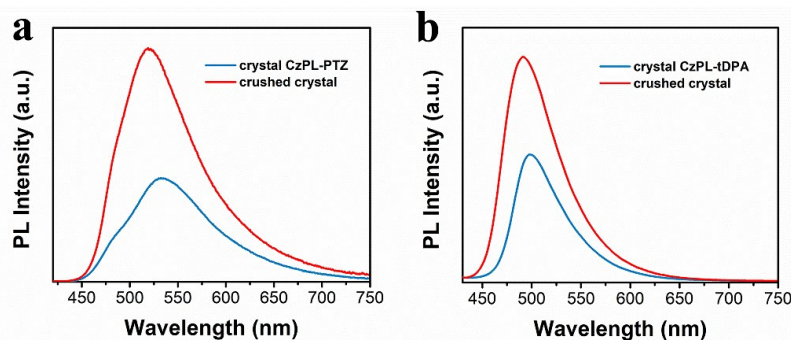


**Figure S11** PL spectra of (a) **CzPL-PTZ** and (b) **CzPL-tDPA** crystals and crushed

crystals.

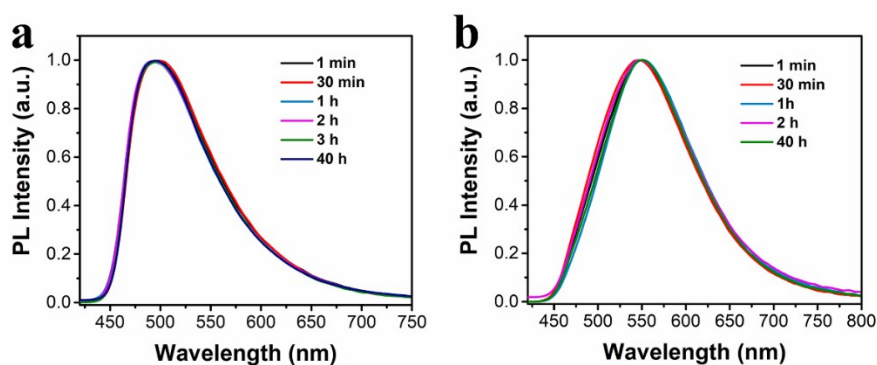


**Figure S12** PL spectra of (a) CzPL-PTZ and (b) CzPL-tDPA ground samples at room temperature after different retention time.

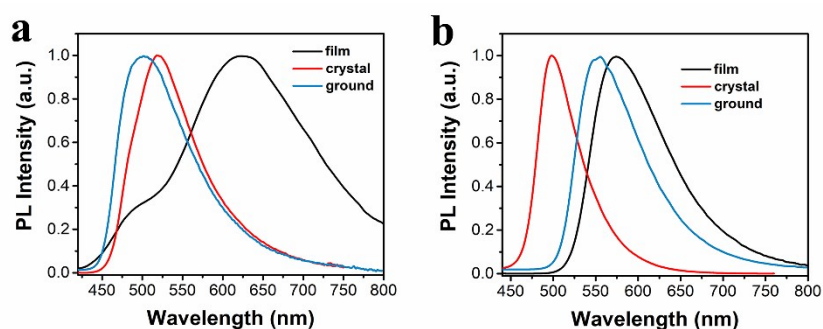


**Figure S13** PL spectra of (a) CzPL-PTZ and (b) CzPL-tDPA in film, crystal and ground samples.

**Table S5** Summary photophysical data of CzPL-PTZ and CzPL-tDPA before and after grinding.

Compound	Crystal (nm)	Crushed crystal (nm)	Ground sample (nm)	Fumed sample (nm)
CzPL-PTZ	533	519	501	520
CzPL-tDPA	498	491	547	518

**Table S6**  $\Phi_f$  values of CzPL-PTZ and CzPL-tDPA before and after grinding.

Compound	Crystal <sup>[a]</sup> (%)	Crushed crystal <sup>[a]</sup> (%)	Ground sample <sup>[a]</sup> (%)
CzPL-PTZ	39	48	35
CzPL-tDPA	66	91	74

[a] Absolute  $\Phi_f$  of crystal, crushed crystal, and ground samples with an integrating sphere at room temperature.

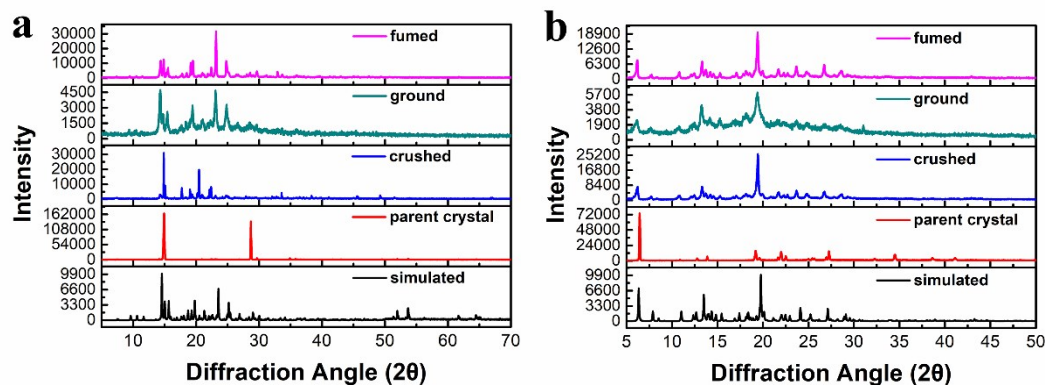


Figure S14 The PXRD patterns of (a) CzPL-PTZ and (d) CzPL-tDPA in simulated crystals, their parent crystals, crushed crystals, ground samples, and fumed samples.

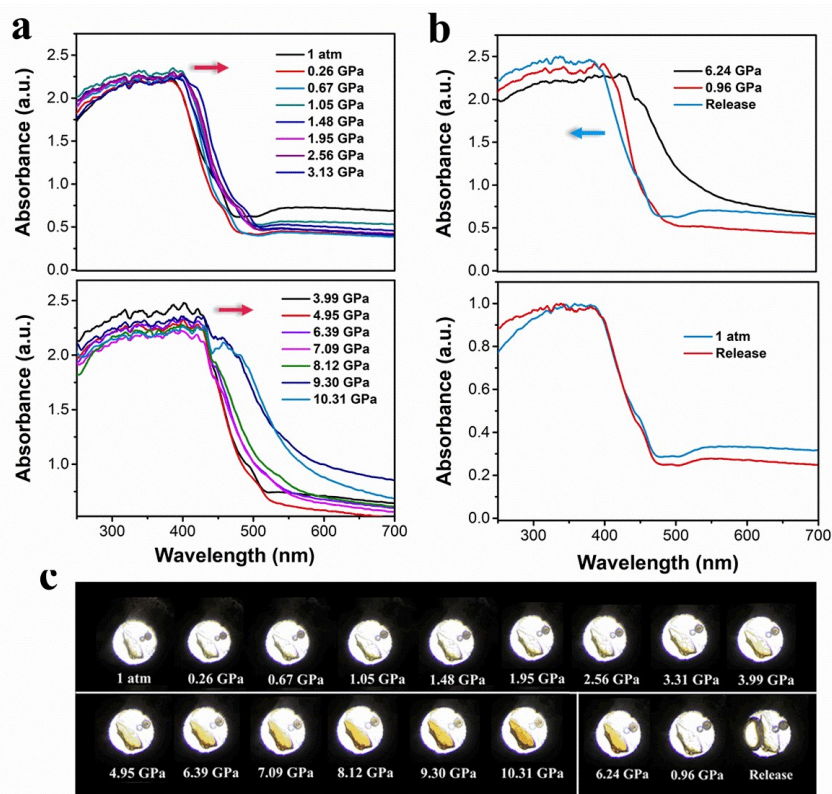
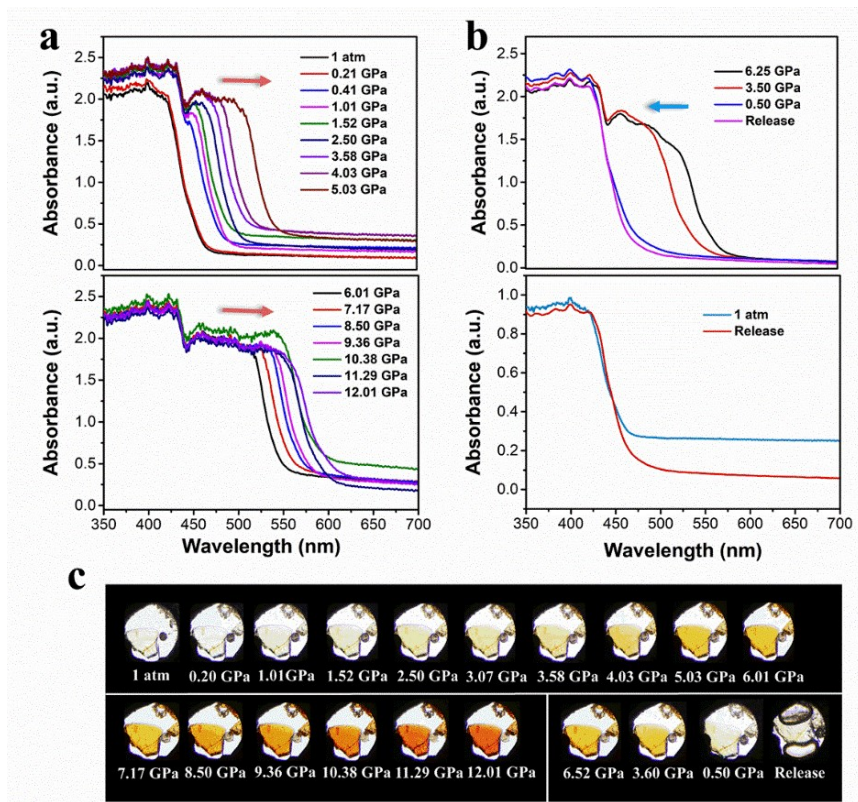
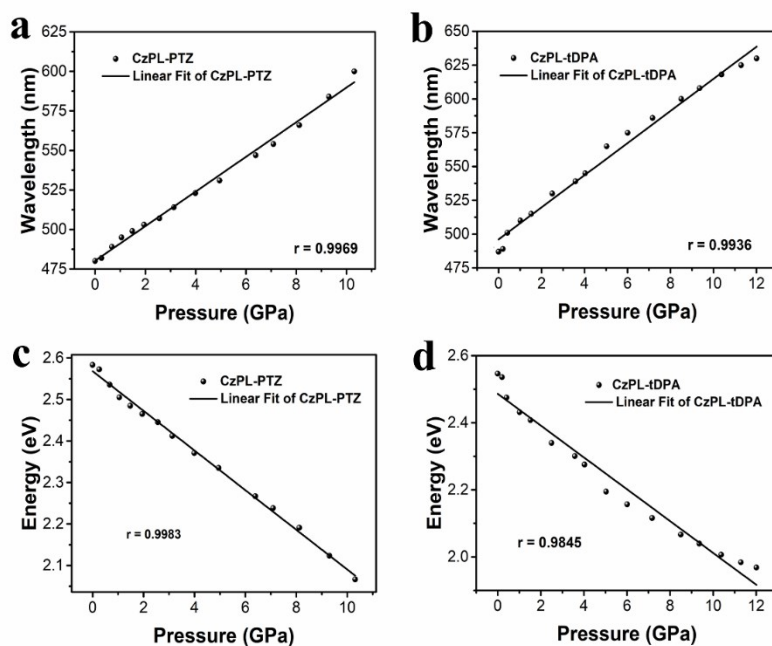


Figure S15 (a) UV-vis spectra of crystal CzPL-PTZ under the pressures from 1 atm to

10.31 GPa, (b) UV-vis spectra of crystal **CzPL-PTZ** during the decompression processes, (c) The visible images of the compressed powder sample under different external pressures.



**Figure S16** (a) UV-vis spectra of crystal **CzPL-tDPA** under the pressures from 1 atm to 12.01 GPa, (b) UV-vis spectra of crystal **CzPL-tDPA** during the decompression processes, (c) The visible images of the compressed powder sample under different external pressures.



**Figure S17** Pressure dependence of emission peaks and emission energy of the crystal (a)(c) **CzPL-PTZ** and (b)(d) **CzPL-tDPA**. Here, the pressure is gradually increasing and r value is expressed as correlation coefficient. The closer r value is to 1, the stronger of the linear correlation between the two variables. In addition, the energy is calculated by the formula  $E=1240/\lambda_{em}$  (eV).

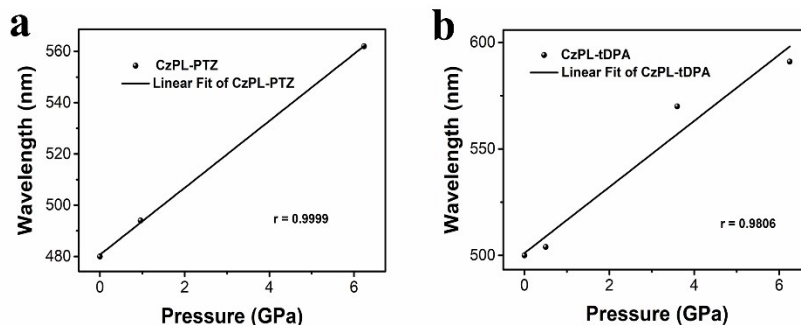


**Figure S18** Pressure dependence of emission peaks of the crystal (a) **CzPL-PTZ** and (b) **CzPL-tDPA**. Here, the pressure gradually decreases.

**Table S7** Summary photophysical data of **CzPL-PTZ** and **CzPL-tDPA** under different external pressures and release of external pressures.

Pressure (GPa)	<b>CzPL-PTZ</b> [UV] (nm)	<b>CzPL-PTZ</b> [PL] (nm)	Pressure (GPa)	<b>CzPL-tDPA</b> [UV] (nm)	<b>CzPL-tDPA</b> [PL] (nm)
0	384	480	0	416	487

0.26	386	482	0.21	420	489
0.67	392	489	0.41	446	501
1.05	396	495	1.01	450	510
1.48	399	499	1.52	453	515
1.95	400	503	2.50	460	530
2.56	405	507	3.58	466	539
3.13	420	514	4.03	480	545
3.99	428	523	5.03	498	565
4.95	432	531	6.01	515	575
6.39	440	547	7.17	525	586
7.09	450	554	8.50	536	600
8.12	455	566	9.36	540	608
9.30	460	584	10.38	545	618
10.31	475	600	11.29	549	625
6.24	427	562	12.01	560	630
0.96	400	494	6.25	515	591
release	380	480	3.60	483	570
			0.50	422	504
			release	421	500

---

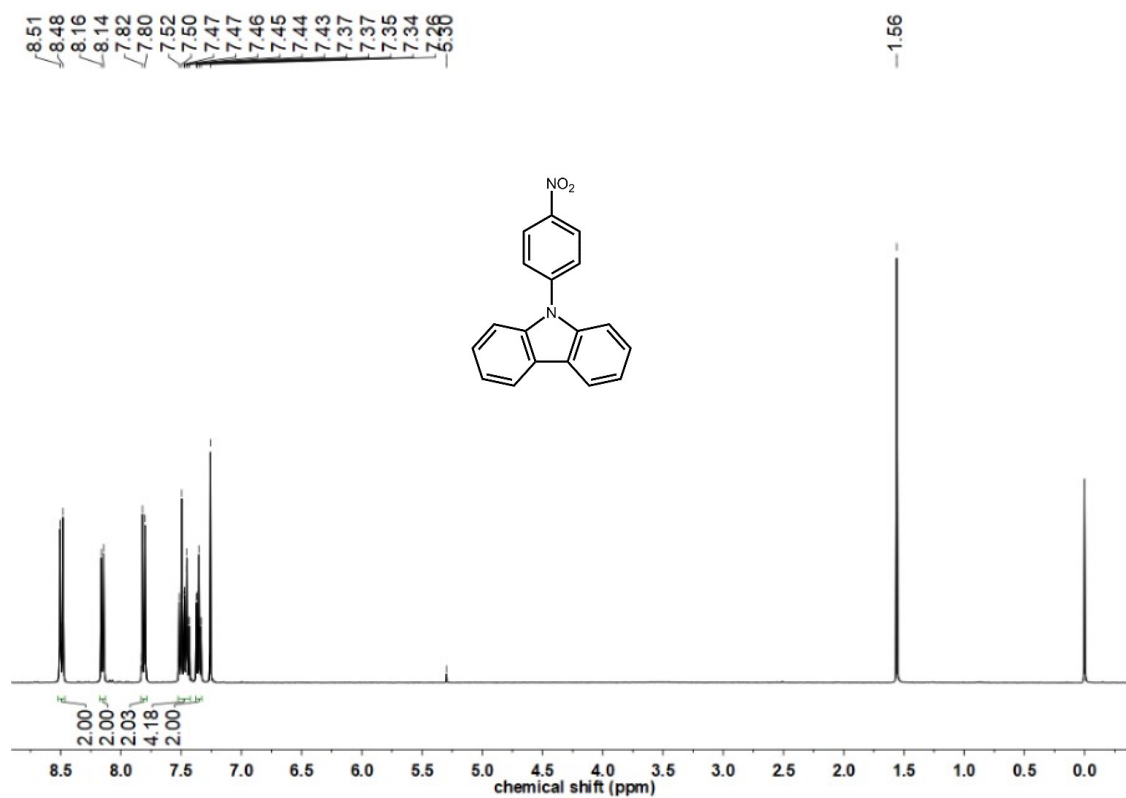


**Figure S19** <sup>1</sup>H NMR spectrum of compound CzPhNO<sub>2</sub> measured in CDCl<sub>3</sub>.

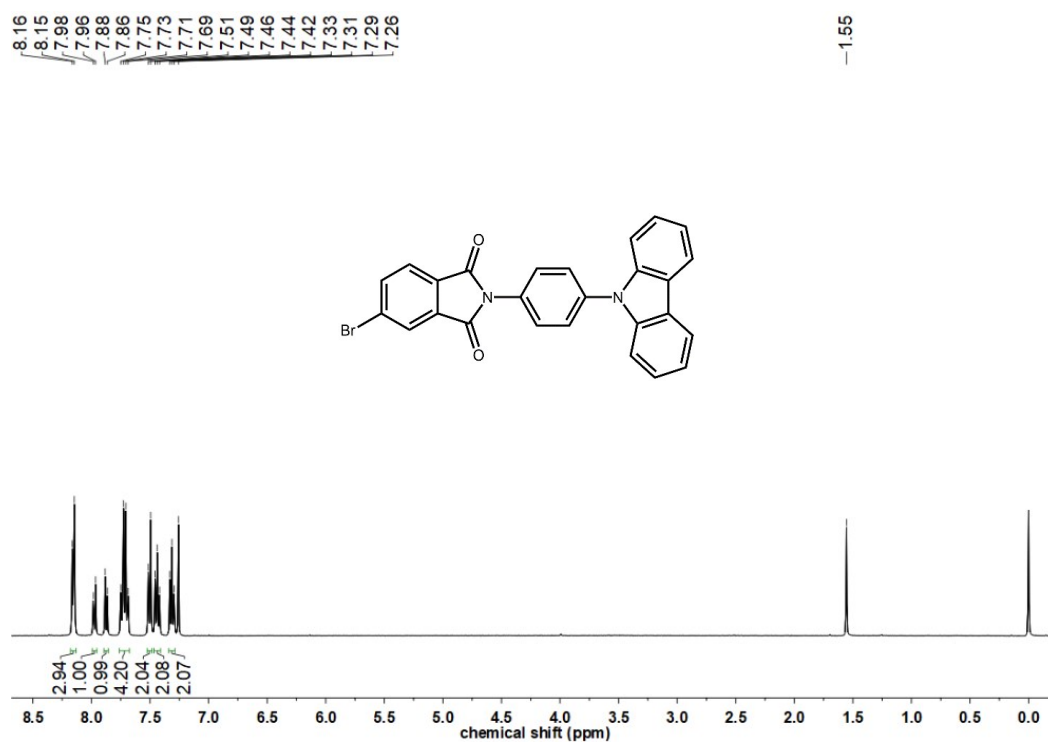


**Figure S20** <sup>1</sup>H NMR spectrum of compound CzPL-Br measured in CDCl<sub>3</sub>.

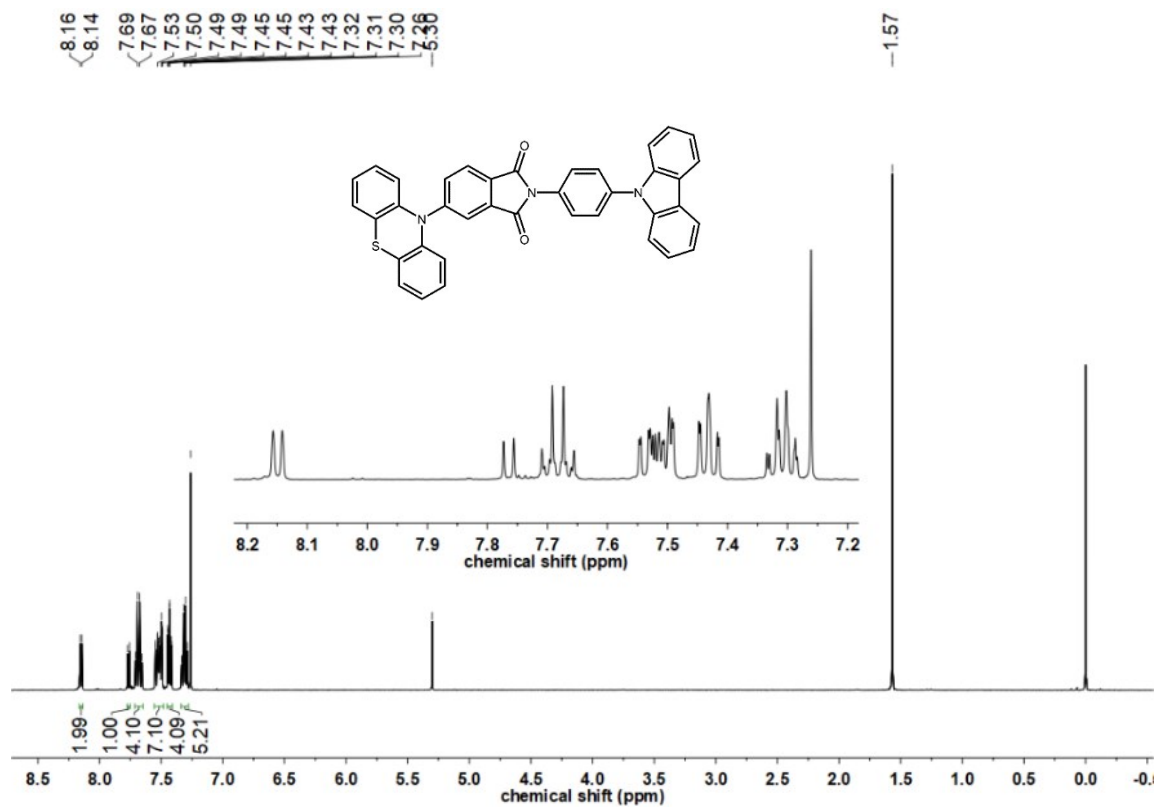


Figure S21  $^1\text{H}$  NMR spectrum of compound CzPL-PTZ measured in  $\text{CDCl}_3$ .

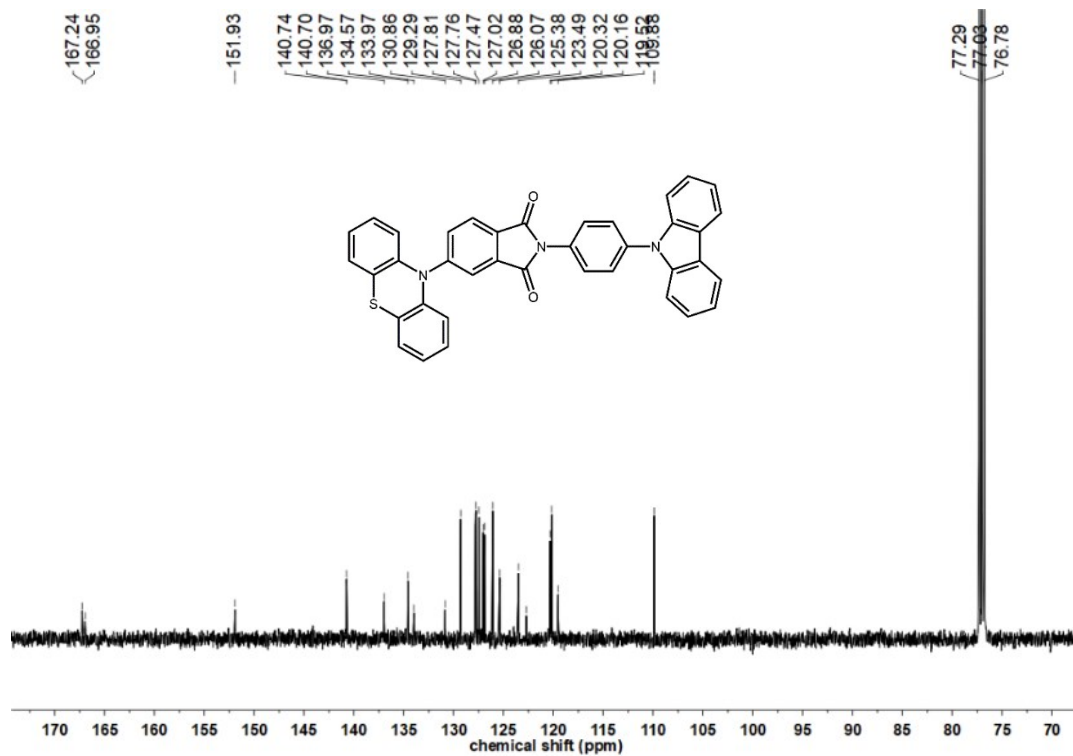
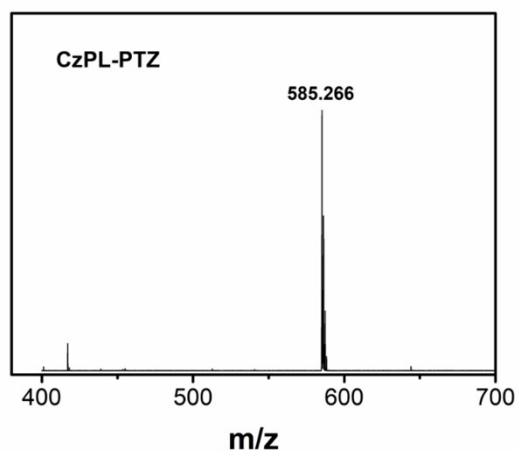
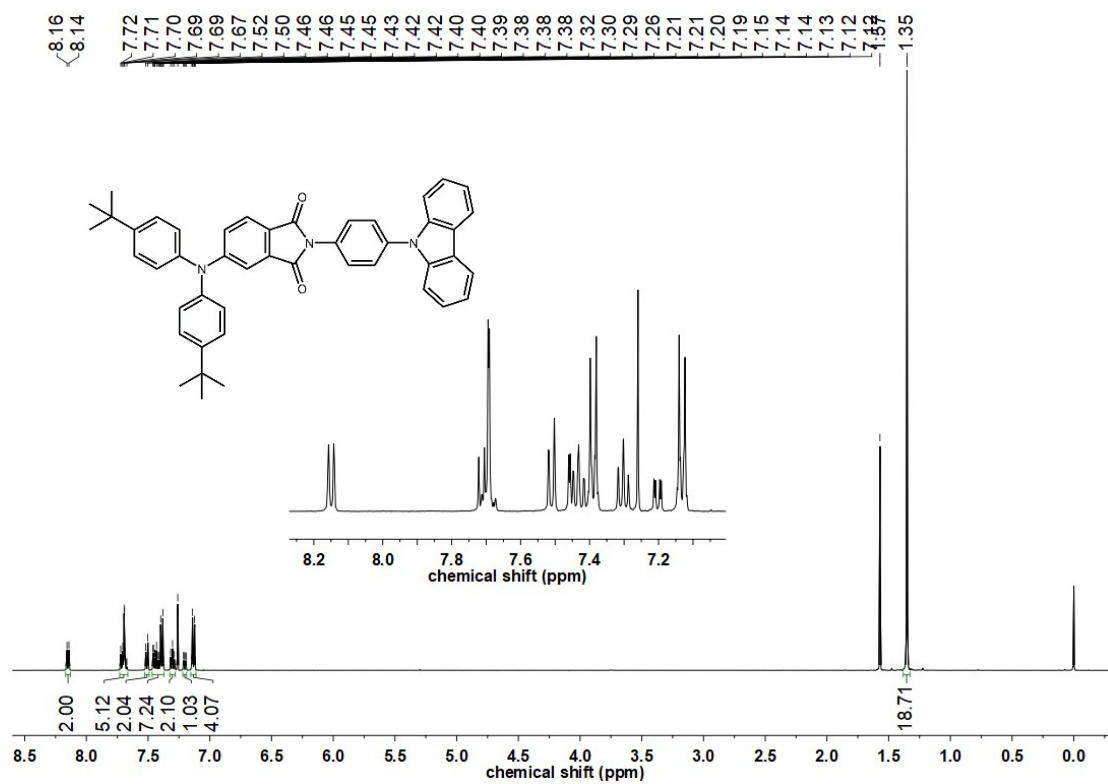


Figure S22  $^{13}\text{C}$  NMR spectrum of compound CzPL-PTZ measured in  $\text{CDCl}_3$ .



**Figure S23** TOF-MS of compound **CzPL-PTZ**.



**Figure S24** <sup>1</sup>H NMR spectrum of compound **CzPL-tDPA** measured in CDCl<sub>3</sub>.

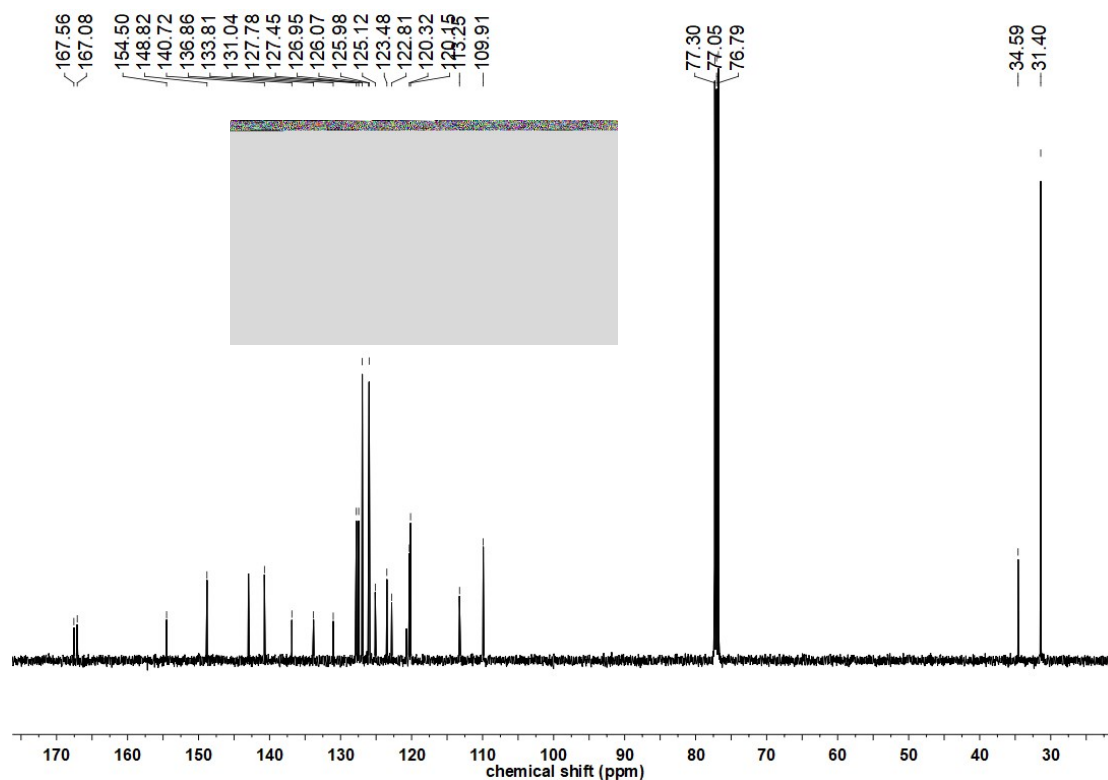


**Figure S25**  $^{13}\text{C}$  NMR spectrum of compound **CzPL-tDPA** measured in  $\text{CDCl}_3$ .

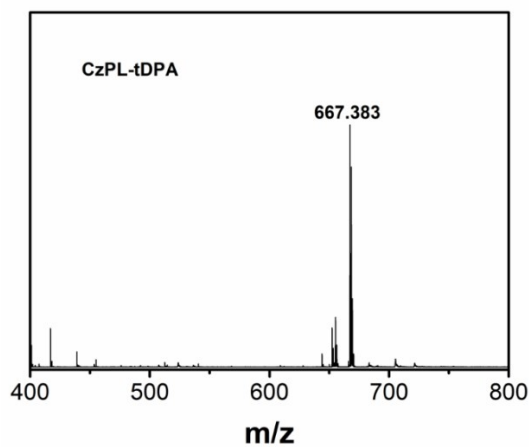


**Figure S26** TOF-MS of compound **CzPL-tDPA**.

#### 4. References

1. H. Zhao, Z. Wang, X. Cai, K. Liu, Z. He, X. Liu, Y. Cao and S.-J. Su, *Mater. Chem. Front.*, 2017, **1**, 2039-2046.
2. C. M. Cardona, W. Li, A. E. Kaifer, D. Stockdale and G. C. Bazan, *Adv. Mater.*, 2011, **23**, 2367-2371.